JOURNAL OF CATALYSIS 88, 26–36 (1984)

Surface Characterization of Thorium–Nickel Intermetallic Catalysts

TUAN A. DANG,* LEONIDAS PETRAKIS,† CHARLES KIBBY,† AND DAVID M. HERCULES*

*Department of Chemistry, University of Pittsburgh, Pittsburgh, Pennsylvania 15260 and †Gulf Research and Development Company, Pittsburgh, Pennsylvania 15230

Received July 29, 1983; revised January 20, 1984

Electron spectroscopy for chemical analysis (ESCA), Auger electron spectroscopy (AES), and ion scattering spectroscopy (ISS) have been used to study a series thorium–nickel alloys (Th_7Ni_3, ThNi, $ThNi_2$, $ThNi_5$), both untreated and treated with different gases (O_2, air, CO/H_2). ESCA results indicate that the surfaces of untreated alloys are Ni-poor with respect to the bulk. Treatment of these alloys with synthesis gas (CO/H_2), O_2, or air results in decomposition of the intermetallic into Ni/ThO_2 or NiO/ThO_2. In all cases Ni was observed to segregate to the surface after reaction. The degree of Ni surface segregation is not affected by different gas treatments but varies for different alloys. The relationship between the relative Ni signal intensity and the bulk Ni content was examined and compared by ESCA, AES, and ISS which have different sampling depths. Catalysts with large surface concentrations of Ni generally show high activity for the methanation reaction. Comparison of the Ni surface concentration with catalytic activity of Th_7Ni_3 and $ThNi_5$ has shown that they do not correlate mathematically. This incompatibility can be explained by the presence of different active sites, a spongy model, or both.

INTRODUCTION

A new class of supported catalysts has been developed (*1–4*) recently which possesses higher activity than conventional supported catalysts prepared by wet chemical techniques. The new catalysts are formed by reaction of synthesis gas (CO/H_2) or O_2 with a binary intermetallic compound which generally consists of a rare earth or actinide element and a first-row transition metal. This conversion may be expressed by

$$ThNi_5 \xrightarrow[CO/H_2]{O_2} Ni/ThO_2,$$

yielding a thoria-supported Ni catalyst. Compounds involving Fe, Co, and Ni with Al or Si (*5, 6*) also have been studied. Among the combinations investigated, the Th–Ni system seems to work best for the methanation reaction. Activity studies have shown (*7, 8*) that the relative methanation activities of catalysts derived from the alloys are $ThCo_5 < ThNi_5 > UNi_5 > ZrNi_5$.

Electron spectroscopy for chemical analysis (ESCA) (*8–12*), and Auger electron spectroscopy (AES) (*7, 13, 14*) have been used to study a number of intermetallic alloy systems. However, no extensive investigation by a combination of several surface techniques has been reported for a single system of alloy catalysts. This type of study has proved to be valuable for studying conventional supported catalysts (*15, 16*). In the present work, we report the use of ESCA, AES, and ion scattering spectroscopy (ISS) to examine a series of Th_xNi_y intermetallic alloys (Th_7Ni_3, ThNi, $ThNi_2$, $ThNi_5$). The investigation included surface characterization of fresh alloys and those treated with different reactive gases (O_2, air, CO/H_2). Catalytic activity data for the oxidized intermetallic catalysts are given and compared with literature values (*1*). A correlation between the results of surface characterization and catalytic activity is included.

EXPERIMENTAL SECTION

Alloys were prepared by melting a stoichiometric mixture of the metals in a water-cooled copper boat under an atmosphere of purified argon as described by Imamura and

0021-9517/84 $3.00

Wallace (*1*). The intermetallics were then ground and sieved to 80 mesh. Studies of fresh intermetallics were accomplished immediately after grinding to avoid extensive air oxidation. Treatment of these alloys was carried out in a flow-type microreactor under air, O_2 and synthesis gas ($H_2/CO = 3$), respectively. When synthesis gas was used, the crushed catalysts were pretreated with H_2 for 2 h to remove the oxide film. All treatments were carried out at 350°C. X-Ray diffraction analysis of the alloys was performed before and after treatment using a Diano XRD-6 diffractometer.

ESCA studies were carried out using an AEI ES-200A electron spectrometer equipped with an aluminum anode and an AEI DS-100 data system. The spectrometer was operated at 12 kV and 22 mA and the base pressure was below 10^{-8} Torr. The digital data obtained from the DS-100 data system were processed with an Apple II microcomputer. Binding energies were referenced to the Cl*s* line at 284.6 eV. Sealable ESCA probes (*16*) were used to transfer air sensitive samples from the reaction chamber to the spectrometer.

A Physical-Electronics Model 545 Auger electron spectrometer was used to obtain Auger spectra of the alloys. The energy and emission current of the primary electron beam were set at 5 keV and 2 mA, respectively. The base pressure was below 10^{-8} Torr.

ISS studies were carried out using a 3M Model 525 ion scattering spectrometer equipped with a cylindrical mirror analyzer (CMA), to measure the energy of the elastically scattered ions. The instrument was backfilled with ^{20}Ne to 2×10^{-5} Torr after a base pressure below 5×10^{-9} Torr was obtained. The primary ion beam was operated at 2 keV and at a current density of 2×10^{-7} A/cm^2.

Catalytic measurements were obtained for oxygen-treated intermetallics (350°C, 20 h). They were done in a microreactor operating at atmospheric pressure. Prior to each run, a sample mixture (50 mg catalyst + 50 mg ground quartz) was reduced in H_2 at 275°C for 16 h. The catalyst mixture was then cooled to room temperature and chemisorbed with CO in a H_2 stream. After the amount of chemisorbed CO was measured, the catalyst was purged with H_2 and heated to 275°C. Hydrogen gas was then exchanged with a synthesis gas mixture having the composition 10% CO, 89% H_2, 1% Ar. Samples of the product were transferred to a gas chromatograph for detection and measurement.

RESULTS

Untreated Alloys

Surface characterization of the untreated alloys (Th_7Ni_3, ThNi, $ThNi_2$, $ThNi_5$) was done using ESCA and AES. The chemical states of the elements on the surfaces of the fresh alloys were determined by ESCA. Examination of the Ni $2p_{3/2}$, lines shown in Fig. 1, and the Th $4f_{7/2}$ spectra of the original intermetallic compounds indicates the presence of Ni, NiO (Ni $2p_{3/2}$ = 852.2 and 854.5 eV), and ThO_2 (Th $4f_{7/2}$ = 333.6 eV) as major surface species. Quantitative ESCA results were obtained using integrated peak areas for Ni $2p_{3/2}$ and Th $4f_{7/2}$. Estimates of the Ni surface concentrations for the alloys can be obtained from

$$\frac{N_{Ni}}{N_{Th}} = \frac{I_{Ni}}{I_{Th}} \times \frac{\sigma_{Th}}{\sigma_{Ni}} \times \sqrt{\frac{E_{Th}}{E_{Ni}}} \times \frac{D_{Th}}{D_{Ni}} \quad (1)$$

using Scofield photoionization cross sections (*17*), where N = number of atoms, I = intensity (peak area), σ = Scofield photoionization cross section, E = kinetic energy of photoelectron, D = detector efficiency. D increases linearly with E in the AEI instrument (*28*). The Ni surface concentrations are plotted as a function of bulk Ni concentration in Fig. 2. It can be seen that all untreated alloys are Ni-poor on the surface. All points fall below the diagonal line. Nickel increases linearly with increasing bulk concentration and then drastically increases after 67% Ni. The ESCA results were confirmed by AES data. A plot of

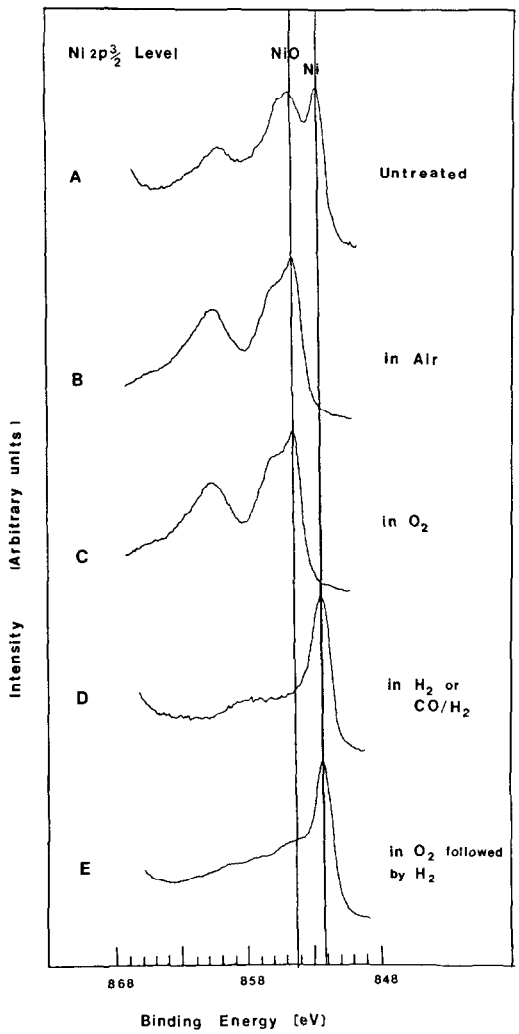

FIG. 1. Ni $2p_{3/2}$ ESCA spectra for $ThNi_5$ with different treatments. ThO_2 was observed in all cases. (A) Untreated. (B) In air (350°C). (C) In O_2 (350°C). (D) Either H_2 or CO/H_2 (350°C). (E) O_2 (350°C) followed by H_2 (400°C).

AES (not shown) relative Ni intensity, Ni/Th + Ni, calculated using peak to peak heights of the Ni $L_3M_{4,5}M_{4,5}$ and the Th $N_7O_5O_5$ lines shows exactly the same trend as the ESCA data.

Treated Alloys

Effect of reactive gases. The effect of reactive gases (O_2, air, CO/H_2) on the alloys was studied in detail. As an example, reduction of $ThNi_5$ in H_2 resulted in surface segregation of Ni. The atomic Ni/Th ratio was found to increase from 2.0 for untreated $ThNi_5$ to 8.8 when the alloy is reduced in H_2 at 350°C for 2 h. Further surface enrichment of Ni was observed when the catalyst was treated with synthesis gas for longer periods (6 h) (Ni/Th = 12.5). The surface of this reacted catalyst consists primarily of metallic nickel (Ni $2p_{3/2}$ = 852.2 eV) and ThO_2 (Th $4f_{7/2}$ = 333.6 eV) (Fig. 1). X-Ray diffraction of the same sample also indicated decomposition of the bulk intermetallic into Ni and ThO_2.

Table 1 shows the effect of O_2 on the surface atomic ratios of $ThNi_5$. The atomic Ni/Th ratio decreased from 2.0 to 1.4 when the sample was oxidized in air for 20 min at 100°C. Longer oxidation times (100°C, 1 h) resulted in an even smaller atomic Ni/Th ratio (0.97). More drastic conditions (200°C, 20 min) caused the bulk intermetallic to decompose into Ni and ThO_2 as observed by X-ray diffraction; under these conditions the atomic Ni/Th ratio began to increase (Ni/Th = 2.9). Higher temperature oxidation (350°C, 1 h) resulted in further decomposition of the intermetallic as well as a further increase in the atomic Ni/Th ratio (Ni/Th = 6.0). Although ThO_2 (Th $4f_{7/2}$ = 333.6 eV) was observed by ESCA for all treatments, the surface Ni was completely

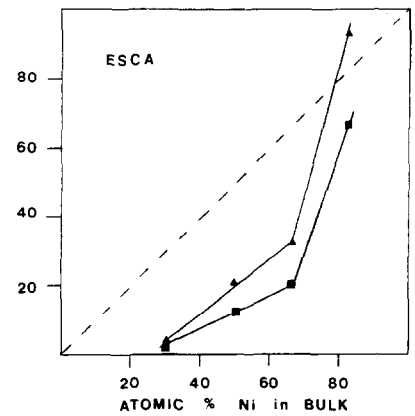

FIG. 2. Relative Ni surface concentration of Th–Ni alloys. (■) Before treatment. (▲) After treatment. The diagonal line indicates equal surface and bulk concentrations.

TABLE 1

Atomic Ratios of $ThNi_5$ for Various Treatments With Air

Treatment	ESCA binding energies,[a] eV		Atomic ratio[b] Ni/Th	Phase(s) (XRD)
	Ni $2p_{3/2}$	Th $4f_{7/2}$		
Untreated	852.2, 854.5	333.6	2.0	$ThNi_5$
In air at 100°C for 20 min	852.2, 854.9	333.6	1.4	$ThNi_5$
In air at 100°C for 60 min	852.2, 854.7	333.6	0.97	$ThNi_5$
In air at 200°C for 20 min	852.2, 854.4	333.6	2.9	$ThNi_5$, Ni, ThO_2
In air at 350°C for 1 h	853.8, 855.6, 861.0	333.6	6.0	$ThNi_5$, Ni, ThO_2, NiO
In air at 350°C for 8 h	853.8, 855.6, 861.0	333.6	13.2	Ni, ThO_2, NiO

[a] Binding energies are measured with a precision of ±0.15 eV.

[b] Atomic ratios are calculated from ESCA data using Scofield photoionization cross section (*17*). Data are measured to ±6% RSD.

oxidized to NiO (Table 1) only at high temperature (350°C, 1 h).

Segregation of Ni to the surface also changed with length of treatment time. Fig. 3 shows a plot of the atomic ratio (Ni/Th) versus oxidation time for $ThNi_5$. A drastic increase in the Ni signal was observed during the first 4 h of oxidation. Further treatment resulted in a small gradual change, reaching a steady state value after about 8 h of oxidation.

The extent of reduction of oxidized $ThNi_5$ was also studied using the "ESCA-H_2 titration" technique (*15, 16*). The oxidized catalysts were reduced in flowing H_2 at 400°C for 4 h and then examined by ESCA without exposure to air. ESCA data showed that surface Ni was completely reduced, as indicated by the appearance of only metallic nickel (Ni $2p_{3/2}$ = 852.2 eV) (Fig. 1).

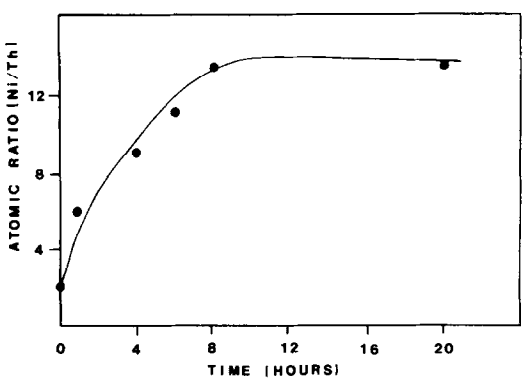

FIG. 3. Change of the Ni/Th atomic ratio with oxidation time for $ThNi_5$ at 350°C.

The effect of oxidation time on other alloys (Th_7Ni_3, ThNi, $ThNi_2$) was also studied. Surface concentrations of Ni for all alloys (Th_7Ni_3, ThNi, $ThNi_2$) were unchanged after 8 h of oxidation. As it can be seen in Table 2, there are no significant differences in atomic Ni/Th ratios whether the alloys were treated for 8 or 20 h. X-Ray diffraction data showed that all alloys were decomposed completely into Ni and ThO_2 after 8 h of oxidation.

Comparison of the effects of different reactive gases on the alloys is shown in Table 2. The results for $ThNi_5$ in Table 2 for reaction with air, O_2, or CO/H_2 show that the Ni/Th atomic ratios are the same for all three treatments within experimental error (±6% RSD). The same effect was observed for the other alloys: Th_7Ni_3, ThNi, and $ThNi_2$. Thus, treatment with different gases results in the same degree of Ni surface segregation. In addition, Table 2 also lists the

TABLE 2

Atomic Ratios of Thorium–Nickel Alloys

Intermetallic	Treatment (350°C)	Atomic ratio[a] Ni/Th	Surface species	Bulk phase (XRD)[b]
Th_7Ni_3	Untreated	0.024	Ni, NiO, ThO_2	Th_7Ni_3
	In CO/H_2 for 6 h[b]	0.026	Ni, ThO_2	Ni, ThO_2
	In O_2 for 8 h	0.027	NiO, ThO_2	Ni, NiO, ThO_2
	In O_2 for 20 h	0.026		
ThNi	Untreated	0.15	Ni, NiO, ThO_2	ThNi
	In H_2/CO for 6 h[b]	0.24	Ni, ThO_2	Ni, ThO_2
	In O_2 for 8 h	0.26	NiO, ThO_2	Ni, NiO, ThO_2
	In O_2 for 20 h	0.26		
$ThNi_2$	Untreated	0.26	Ni, NiO, ThO_2	$ThNi_2$
	In H_2/CO for 6 h[b]	0.42	Ni, ThO_2	Ni, ThO_2
	In O_2 for 8 h	0.44	NiO, ThO_2	Ni, NiO, ThO_2
	In O_2 for 20 h	0.47		
$ThNi_5$	Untreated	2.0	Ni, NiO, ThO_2	$ThNi_5$
	In H_2 for 2 h	8.8	Ni, ThO_2	$ThNi_5$
	In H_2/CO for 6 h[b]	12.5	Ni, ThO_2	Ni, ThO_2
	In air for 8 h	13.2	NiO, ThO_2	Ni, NiO, ThO_2
	In O_2 for 8 h	12.5	NiO, ThO_2	Ni, NiO, ThO_2
	In O_2 for 20 h	13.2		

[a] Atomic ratios are calculated from ESCA data using Scofield photoionization cross section (*17*). Data are measured to ±6 RSD.

[b] All synthesis gas treatments are prereduced in H_2 at 350°C for 2 h.

species found on surfaces of the reacted alloys by ESCA. Ni and ThO_2 were found in alloys decomposed by synthesis gas while NiO and ThO_2 existed on oxidized alloys.

Relationship between relative Ni intensity and bulk concentration. The relationship between relative Ni intensity (Ni/Th + Ni) of the oxygen-reacted catalysts versus bulk Ni content was examined by both ESCA and AES. In the case of ESCA, the relative Ni intensity can be corrected to represent the relative surface concentration of Ni as shown in Fig. 2. Both ESCA and AES show segregation of Ni to the surface when the alloys are treated. Note the unusual enrichment of Ni on the surface of $ThNi_5$ relative to the other Th–Ni alloys which are still Ni poor with respect to the bulk (Fig. 2).

Figure 4 shows ISS spectra of the oxygen-reacted alloys. The Ni signal is weak for Th_7Ni_3, ThNi, and $ThNi_2$, but it is quite significant for $ThNi_5$. A plot of ISS Ni relative intensity (Ni/Th + Ni) versus bulk Ni concentration, shown in Fig. 5, indicates constant relative Ni intensity with increasing bulk Ni content for the first three re-

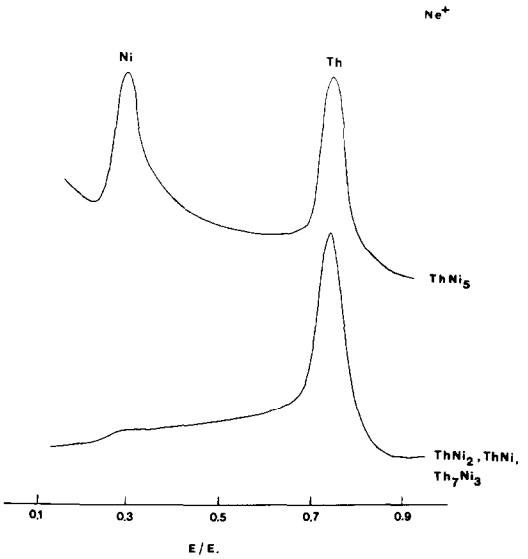

FIG. 4. ISS spectra for oxygen-treated Th–Ni alloys.

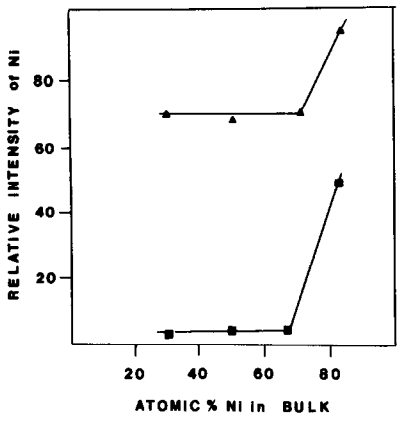

FIG. 5. Relative intensity ratio (Ni/Ni + Th) for oxygen-treated Th–Ni alloys. (■) ISS. (▲) Valence AES.

acted intermetallics, but a significant difference for $ThNi_5$.

Information about the outermost atomic layers of the treated alloys can also be obtained from Auger lines involving valence-electron transitions. There is some overlap between the valence peaks of TH, O_4P_2V (65 eV), and Ni, MVV 61 eV), as shown in Fig. 6. Although peak-to-peak heights of the Ni MVV peak (61 eV) in all four alloys are not much affected by the Th O_4P_2V (65 eV) peak, the converse is not true. The Th O_4P_2V (65 eV) lines of $ThNi_5$ completely overlap the Ni MVV signal (61 eV). Thus, the Th O_5VV peak (81 eV) was used for analysis. A plot of relative Ni intensity, Ni/Th + Ni, using peak-to-peak height of Ni MVV (61 eV) and Th O_5VV (81 eV) versus bulk Ni content (Fig. 5) shows a trend similar to that observed for the ISS data (Fig. 5).

Methanation Reaction

Activity data for oxygen-treated catalysts are summarized in Table 3. Turnover numbers and rates of CO conversion to hydrocarbon are given at 3 and 7 h. All catalysts showed a slight decrease in activity with time on stream. Although $ThNi_5$ was found to be the most active catalyst, rates corrected per gram of Ni decreased rapidly with increasing Ni content (Table 3). The same phenomenon was observed for sorption capacity. As shown in Table 3, CO chemisorption of $ThNi_5$ is larger than that of any other Th–Ni catalyst. However, the metal dispersion derived from sorption data showed a rapid decline with increasing Ni content (Table 3). The calculation was made based on the assumption that one CO molecule interacts with one Ni metal atom (*1*). Methane and ethane were the two main products in CO hydrogenation of Th–Ni catalysts. Their fractions are listed in Table 3. Methane selectivity changes with Ni content. An alloy with higher Ni content generally gives a larger fraction of methane. It is noteworthy that the methane selectivity also increased with time on stream.

The relative Ni surface concentrations of the used catalysts estimated from ESCA data are listed in Table 3. Values for oxidized alloy catalysts are also given for comparison. The relative surface concentrations of Ni in used catalysts were found to be smaller than those of oxidized catalysts,

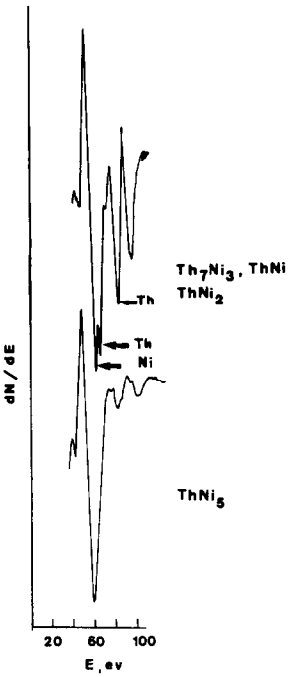

FIG. 6. Valence AES spectra of oxygen-treated Th–Ni alloys.

TABLE 3

Characterization and Activity of Th–Ni Catalysts[a]

Alloy	Th_7Ni_3[b]	ThNi[b]	$ThNi_2$[b]	$ThNi_5$[c]
CO sorption (μmol/g)	42	80	66	98
Overall dispersion (%)	2.9	2.7	1.3	1.2
CO conversion rate (cm^3/g/sec)				
3 h	5.8×10^{-2}	7.2×10^{-2}	5.2×20^{-2}	12×10^{-2}
7 h	4.9×10^{-2}	5.1×10^{-2}	3.6×10^{-2}	9.6×10^{-2}
Normalized rate[d] (cm^3/g Ni/sec)				
3 h	0.68(0.67)	0.42(0.40)	0.18(0.17)	0.26(0.23)
7 h	0.57(0.56)	0.30(0.28)	0.13(0.12)	0.21(0.18)
Turnover number (sec^{-1})				
3 h	0.061	0.042	0.035	0.054
7 h	0.051	0.029	0.025	0.044
Fraction of methane formed (%)				
3 h	83	85	85	86
7 h	85	86	87	87
Fraction of ethane formed (%)				
3 h	17	15	15	14
7 h	15	14	13	13
Relative surface concentration of Ni (%)				
Oxidized	2.5	21	32	96
Used	1.3	12	15	87

[a] $H_2/CO = 9$, Rates obtained at 275°C.
[b] Treated in O_2 for 20 h at 350°C.
[c] Treated in O_2 for 16 h at 350°C. Temperature was raised slowly to avoid sintering.
[d] Assume decomposition products are NiO/ThO_2 and Ni/ThO_2 for values in parentheses.

which suggests that some sintering has occurred in the used catalysts.

DISCUSSION

Untreated Alloys

Magnetic (*11*) and ESCA (*9*) investigations of $LaNi_5$ have shown that exposure of $LaNi_5$ to low levels of O_2 results in surface segregation of La to form La_2O_3, along with precipitation of Ni to form superparamagnetic metallic Ni particles. Surface segregation of Th as well as oxidation of Th and Ni have been observed by Schlapbach and Brundle (*9*) in an ESCA study of $ThNi_5$ when this alloy is oxidized mildly (10^9 L O_2). Transformations similar to those of $LaNi_5$ would be expected for $ThNi_5$ because of similarities between the two systems.

In the present study, the untreated alloys have been oxidized by exposure to air at room temperature, which corresponds to more severe oxidizing conditions than those used by Schlapbach and Brundle (*9*). Thus, the surface transformation of the alloys discussed above and the consequences, such as an Ni-poor surface with respect to the bulk and the existence of ThO_2, Ni, and NiO as surface species, were observed.

Treated Alloys

The Th–Ni alloys were decomposed by all of the reactive gases studied: air, O_2, and CO/H_2. In the cases of O_2 and air, it is suggested that (*1*) oxygen reacts selectively with thorium to form ThO_2 due to the strong affinity of thorium for oxygen ($\Delta H_f = -292$ kcal/g mol). This results in precipitation of Ni from the original intermetallic, which will then segregate to the surface. An analogous mechanism should be expected for CO since it has been shown (*19*) that CO is dissociated into C and O in the methana-

tion reaction. This dissociated O should affect the Th–Ni alloys in a similar manner to regular oxygen.

Comparison of relative Ni surface concentrations of all alloys under different gas treatments has shown that they are the same within experimental error (±6 RSD). Since Ni is the catalytically active species in the methanation reaction, activities of the alloy catalysts are expected to be similar whether they are formed by treatment with air, O_2, or CO/H_2. Indeed, the activity data for the methanation reaction of oxidized $ThNi_5$ and $ThNi_5$ decomposed by synthesis gas, show that they are not very different (*1*). Similar activities were also observed for Ni–Si and Co–Si (*5*) alloys, decomposed by either O_2 or CO/H_2.

The extent of Ni reduction studied by the ESCA–H_2 titration technique has been valuable for detecting the presence of metal–support interactions in conventional supported catalysts. For example, in γ-alumina-supported catalysts (*15*) only part of the surface Ni is reducible. This can be explained by formation of two Ni species on the surface: "readily reduced Ni" and "hard to reduce Ni," which have been assigned as NiO and a "surface aluminate," respectively. Results from the ESCA–H_2 titration of oxidized $ThNi_5$ show that all of the surface Ni is reduced by H_2 (Fig. 1D). The existence of both NiO (Ni $2p_{3/2}$ = 853.8 and 855.6 eV) on oxidized $ThNi_5$ and the facile reducibility of the Ni species (Fig. 1) indicate that there is essentially no interaction between the transition metal and the support in Th_xNi_y intermetallic catalysts. It is noteworthy that ESCA–H_2 titration measurements have also been performed on Ni/ThO_2-supported catalysts (*20*) prepared by conventional impregnation methods. No metal–support interaction was observed for the conventional thoria-supported Ni catalysts.

Relationship between relative Ni intensity and bulk concentration. Examination of the relative intensity of an element versus its bulk concentration has been valuable

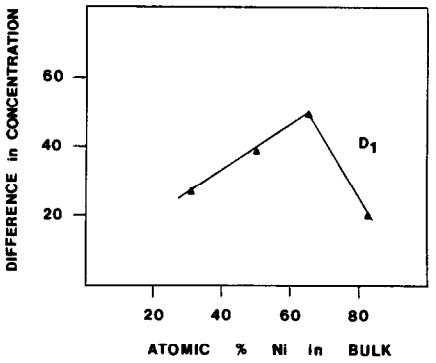

FIG. 7. Change in concentration of thorium–nickel alloys. D_1 = Difference between bulk and surface concentration of Ni fresh alloys $[(N_{Ni}/N_{Ni} + N_{Th})_{bulk} - (N_{Ni}/N_{Ni} + N_{Th})_{surface}]$.

for detecting changes in surface properties of alloy systems as the composition is changed (*21*). Such differences are usually indicated by observing changes in the slope of a plot of relative intensity vs bulk composition. Plots of both ESCA (Fig. 2) and AES relative Ni intensities of fresh alloys versus bulk Ni concentration show a discontinuity at 67% Ni. This suggests a surface property change when the Ni concentration is increased beyond 67%.

As was discussed in previous sections, exposure of the fresh alloys to air caused transformation of the alloy surface to Ni, NiO/ThO_2 along with the segregation of thorium to the surface, which subsequently results in an Ni poor surface relative to the bulk. The degree of transformation depends on temperature and the stability of the alloy. At room temperature, a less stable alloy would undergo surface transformation more readily and surface segregation of thorium more extensively. As a consequence, a smaller Ni surface concentration compared to the bulk is obtained, which gives rise to a larger difference between bulk and surface concentrations of Ni. Thus, a plot of Ni concentration difference between the bulk and surface of the fresh alloys: $D_1(D_1 = N_{Ni}/(N_{Ni} + N_{Th})_{bulk} - N_{Ni}/(N_{Ni} + N_{Th})_{surface}$, versus bulk Ni content (Fig. 7) would give information regarding

the stability of the alloys. As shown in Fig. 7, D_1 increases linearly with bulk Ni content and then drastically decreases for $ThNi_5$. This suggests that except for $ThNi_5$ which is unusually stable, an alloy with larger Ni content would be less stable. It is also noteworthy that $ThNi_2$ and ThNi are found to be less stable than Th_7Ni_3 and $ThNi_5$. This has also been reported by Imamura and Wallace (*1*) who observed that $ThNi_2$ and ThNi are readily decomposed at room temperature while Th_7Ni_3 and $ThNi_5$ are decomposed completely only at 350°C.

ESCA (*22*) and AES (*23*) generally give information about 10–20 atomic layers while ISS (*24*) is considered to be sensitive to the first one or two atomic layers. Examination of ESCA (Fig. 2) and AES data for treated alloys (not shown) indicates that for the top 10–20 atomic layers, Ni concentration increases with bulk Ni content and an unusual accumulation of Ni relative to the other Th–Ni alloys is observed for $ThNi_5$. It is noteworthy that except for $ThNi_5$ the surfaces of even the reacted catalysts are still Ni poor with respect to the bulk (Table 2). The large enrichment of Ni on the surface of treated $ThNi_5$ is again shown in ISS results (Fig. 5). However, Ni concentrations in the first atomic layers of the other three treated alloys are essentially unchanged and are significantly lower than $ThNi_5$. ISS results are also confirmed by valence AES data as shown in Fig. 5.

Methanation Reaction

CO chemisorption and activity data for the methanation reaction of Th_xNi_y catalysts are in general agreement with those reported by Imamura and Wallace (*1*). Similar variations in CO sorption and activity with bulk Ni content were obtained. $ThNi_5$ was the most active catalyst while the other three alloys Th_7Ni_3, ThNi, and $ThNi_2$ showed comparable activity with each other (Table 3).

Comparison between our results for Th_xNi_y intermetallic catalysts and those of 5% Ni supported on alumina has shown that only $ThNi_5$ is more active than the alumina-supported catalyst. CO chemisorption and turnover number for total conversion at 275°C of 5% Ni/Al_2O_3 were found to be 110 μ mol/g and 0.038/sec, respectively. The corresponding rate is 9.5×10^{-2} $cm^3/g/sec$. $ThNi_5$ showed lower sorption capacity (97 μmol/g) but a higher CO conversion rate (12×10^{-2} $cm^3/g/sec$) and turnover number (0.054 sec^{-1}).

Surface Characterization and Methanation Activity of Th_xNi_y Alloys

Comparison of the surface analysis and activity (Table 3) shows that there is some interdependence between the surface concentration of Ni and activity; high Ni surface concentration generally results in greater methanation activity. For example, the high activity of $ThNi_5$ relative to other Th–Ni alloys can be explained by the large enrichment of surface Ni (Table 3). The similar activities of Th_7Ni_3, ThNi, and $ThNi_2$ can be accounted for by the equivalent Ni intensity of those three alloys detected by ISS and valence band AES. However, a quantitative correlation between activity and surface concentration of Ni in Th_7Ni_3 and $ThNi_5$ has shown that while the activity of $ThNi_5$ is twice that of Th_7Ni_3, the relative surface concentration of $ThNi_5$ is 30 times larger than that of Th_7Ni_3. This inconsistency can possibly be explained by the presence of different types of active sites. It is possible that thorium could play an active role in the methanation reaction in addition to its function as a dispersing agent. Thorium has been used as a promoter in several types of reactions. Since thorium content in Th_xNi_y alloys decreases with increasing Ni concentration, the amount of Th which is available for incorporation with Ni in $ThNi_5$ is very much less than that of Th_7Ni_3. Thus, there are possibly two types of Ni in $ThNi_5$. The active Ni which is tightly interacted with thorium and the less active one which is surrounded by Ni itself. Since surface techniques (ESCA, AES, ISS) cannot differentiate different

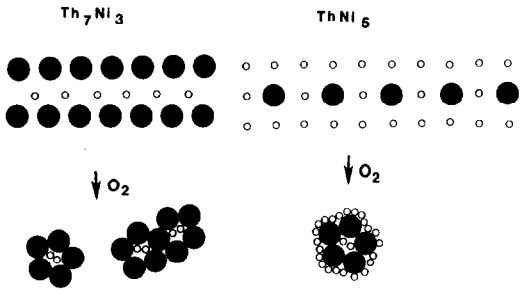

FIG. 8. Models for thorium–nickel catalysts. (●) Th or ThO_2. (○) Ni or NiO.

types of Ni species, the large surface concentration of Ni in $ThNi_5$ can be misleading.

The lack of correlation between Ni surface concentration and the activities of Th_7Ni_3 and $ThNi_5$ also can be interpreted by considering that some Ni in Th_7Ni_3 is covered by ThO_2 and therefore cannot be detected by ESCA. This "unseen Ni," however, must chemisorb CO and be reactive (Table 3). It is suggested that some type of aggregate is formed as a result of oxidation; a possible type of aggregate is shown in Fig. 8. The clusters are composed of ThO_2 which forms a cover and Ni which fills the pores. Any excess Ni will be on top of the ThO_2 cover. This cover of ThO_2 is probably spongy and can be penetrated by hydrogen as well as CO. Thus, Ni under this permeable ThO_2 layer is readily reacted and can chemisorb CO.

In the case of $ThNi_5$, the same model can apply. Since $ThNi_5$ is a Ni-rich compound, it is likely that Ni will be deposited on top of ThO_2 spongy layers. This effect will result in a large accumulation of Ni on the surface. Models for ThNi and $ThNi_2$ should resemble both Th_7Ni_3 and $ThNi_5$, but should be more analogous to Th_7Ni_3 because the Ni concentrations at the surfaces of ThNi and $ThNi_2$ are smaller than those of the bulk and they are equivalent to that of Th_7Ni_3 (Fig. 5). Although our data do not permit exact distinction between the two models suggested, we believe that the second (as shown in Fig. 8) is the more likely.

SUMMARY

1. Untreated alloys have already undergone surface transformation into Ni, NiO, and ThO_2. All are Ni-poor on the surface with respect to the bulk.

2. Treatment of the alloys with CO/H_2, air, or O_2 results in both surface and bulk decomposition of the original intermetallic into either Ni/ThO_2 or NiO/ThO_2.

3. In all cases, Ni is observed to segregate to the surface when the intermetallics are treated. The degree of segregation is found to be the same for different reactive gases.

4. Catalysts with high surface concentrations of Ni generally show greater methanation activity. Lack of a quantitative correlation between the activity and surface Ni concentration of Th_7Ni_3 and $ThNi_5$ is probably due to different types of $Ni–ThO_2$ aggregates being formed in the Ni-poor (Th_7Ni_3) and Ni-rich ($ThNi_5$) alloys.

ACKNOWLEDGMENTS

This work was supported in part by the National Science Foundation under Grant CHE80-20001. We thank Dr. Marwan Houalla for helpful discussions.

REFERENCES

1. Imamura, H., and Wallace, W. E., *J. Catal.* **65,** 127 (1980).
2. Wallace, W. E., Elattar, A., Imamura, H., Craig, R. S., and Moldovan, A. G., *in* "Science and Technology of Rare Earth Material" (Wallace, W. E., and Subbarao, E. C., Eds.), p. 329. Academic Press, New York, 1980.
3. Luengo, C. A., Cabrera, A. L., Mackay, H. B., and Maple, M. B., *J. Catal.* **47,** 1 (1977).
4. Baglin, E. G., Atkinson, G., and Nicks, L., *Ind. Eng. Chem. Prod. Res. Dev.* **20,** 87 (1981).
5. Imamura, H., and Wallace, W. E., *J. Phys. Chem.* **83,** 2009 (1979).
6. Imamura, H., and Wallace, W. E., *J. Phys. Chem.* **83,** 3261 (1979).
7. Moldovan, A. G., Elattar, A., Wallace, W. E., and Craig, R. S., *J. Solid State Chem.* **25,** 23 (1978).
8. Chin, R., Elattar, A., Wallace, W. E., and Hercules, D. M., *J. Phys. Chem.* **84,** 2895 (1980).
9. Schlapbach, L., and Brundle, C. R., *J. Phys.* (Orsay, Fr.) **42,** 1025 (1981).

10. Schlapbach, L., *Solid State Commun.* **38,** 117 (1981).
11. Schlapbach, L., Stucki, F., Sieler, A., and Siegmann, H. C., *Surf. Sci.* **106,** 157 (1981).
12. Siegmann, H. C., Schlapbach, L., and Brundle, C. R., *Phys. Rev. Lett.* **40,** 97, 2 (1980).
13. Von Waldkirch, T., and Zurcher, P., *Phys. Lett.* **33,** 689 (1978).
14. Berry, C., Majumdar, D., and Chung, Y. W., *Surf. Sci.* **94,** 293 (1980).
15. Wu, M., and Hercules, D. M., *J. Phys. Chem.* **83,** 2003 (1979).
16. Ng, K. T., Hercules, D. M., *J. Phys. Chem.* **80,** 1094 (1976).
17. Scofield, J. H., *J. Electron Spectrosc. Relat. Phenom.* **8,** 129 (1976).
18. Veal, B. W., and Lam, D. J., *Phys. Rev. B* **10,** 4902 (1976).
19. Zagli, A. E., Falconer, J. L., and Keenan, C. A., *J. Catal.* **56,** 453 (1979).
20. Shyu, J. Z., and Hercules, D. M., unpublished results, University of Pittsburgh, 1983.
21. Klein, J. C., and Hercules, D. M., *Anal. Chem.* **53,** 754 (1981).
22. Riggs, W. M., and Parker, M. J., *in* "Methods of Surface Analysis" (Czánderna, A. W., Ed.), Chap. 4. Elsevier, New York, 1975.
23. Joshi, A., Davis, L. E., and Palmberg, P. W., Methods of Surface Analysis; (Czanderna, A. W., Ed.), Chap. 5. Elsevier, New York, 1975.
24. Buck, T. M., *in* "Methods of Surface Analysis" (Czanderna, A. W., Ed.), Chap. 3. Elsevier, New York, 1975.
25. Tauster, S. J., Fung, S. C., and Garten, R. L., *J. Amer. Chem. Soc.* **100,** 170 (1978).
26. Fung, S. C., *J. Catal.* **76,** 225 (1982).
27. Vanice, M. A., *J. Catal.* **37,** 449 (1975).
28. Barrie, A., "Handbook of X-Ray and Ultraviolet Photoelectron Spectroscopy" (Briggs, D., Ed.), p. 116. Heyden, London, 1977.